FOREX Publication
Open Access | Rapid and quality publishing

International Journal of
Electrical and Electronics Research (IJEER)
Research Article | Volume 13, Issue 1 | Pages 171-177 | e-ISSN: 2347-470X

Enhanced Luo Converter for Low Component Stress in DC-DC Power Conversion for Fuel Cell Powered BLDC Motor Drive

Teja Sreenu Tadivaka[1], M Kiran Kumar[1], G. Rami Reddy[2], Ch. Rami Reddy[3,4]

[1]*Department of Electrical and Electronics Engineering, Koneru Lakshmaiah Education Foundation, Vaddeswaram – 522302, India. tejasreenu.tadivaka@gmail.com, kiran.malligunta@gmail.com*

[2]*Department of Mathematics, Malla Reddy Engineering College, Secunderabad – 500100, India. dr.g.ramireddy76@gmail.com*

[3]*Department of Electrical and Electronics Engineering, Joginpally B R Engineering College, Hyderabad – 500075, India*

[4]*Applied Science Research Center, Applied Science Private University, Amman-11937, Jordan; crreddy229@gmail.com*

*__Correspondence:__ Ch. Rami Reddy; *crreddy229@gmail.com*

ABSTRACT- Fuel cell powered BLDC motor drive for electric vehicle is the cleaner energy conversion solution with higher efficiency. DC-DC power conversion in this drive plays a significant role in adoptability, efficiency and reliability of the overall drive. This paper presents an enhanced Luo converter for increased voltage gain with additional multiplier stage and reduced capacitor voltage stress owing to reduced clamping voltage. The topology, operational modes, and mathematical analysis of the proposed power conversion are presented. Simulation is carried out in MATLAB/SIMULINK platform which analyzed operational parameters such as output voltage ripple, output voltage regulation, converter components voltage stress, and inductor current ripple. Also, the proposed converter structural advantages are compared to existing converters. The findings on operational and structural parameters resulted in stringent output regulation less than 1 percent for desired output voltage. Also, 41.67 percent reduction is observed for voltage stress across converter capacitors. Thus, an enhanced Luo DC-DC power conversion is designed and validated for fuel cell powered BLDC motor-based EV drive.

Keywords: Fuel cell, FCEV, Boost converter, Luo converter, voltage stress, PI controller.

ARTICLE INFORMATION

Author(s): Teja Sreenu Tadivaka, M Kiran Kumar, G. Rami Reddy, Ch. Rami Reddy;

Received: 23/10/2024; **Accepted**: 19/02/2025; **Published**: 30/03/2025;
e-ISSN: 2347-470X;
Paper Id: IJEER 2310-22;
Citation: 10.37391/ijeer.130122
Webpage-link:
https://ijeer.forexjournal.co.in/archive/volume-13/ijeer-130122.html

Crossref member — CROSSREF.ORG THE CITATION LINKING BACKBONE

Publisher's Note: FOREX Publication stays neutral with regard to Jurisdictional claims in Published maps and institutional affiliations.

1. INTRODUCTION

Hydrogen Fuel cell-powered vehicles contribute to clean energy along with high energy density in producing efficient electric power. The use of brushless direct current (BLDC) motors is widespread is due to its excellent efficiency, wide speed range, and great torque for their size of motor making it suitable for electric vehicle (EV) applications. The DC-DC step-up converter with an extensive voltage-gain is crucial in power conversion of fuel cell powered drive. The usage of traditional boost DC-DC converter is obsolete in these systems owing to the requirement of higher duty cycles for higher voltage gain. Also, the high DC bus voltage is additional high- voltage stress on converter components in conventional boost converter. Therefore, various topologies have been suggested by researchers to develop a high voltage gain and low voltage stress in a DC- DC boost conversion. Additionally, the size and efficiency of the power conversion determine the adoptability, and reliability of the overall drive. Following provides the review of existing power conversion methodologies in this respect.

The Z-source cascade switching capacitor DC-DC converter has been presented without using any further switches that are active, the suggested converter expands the range of boost factors [1-2]. Different Z-source DC-DC converter types can use the suggested converter. The boost factor theoretical values have been compared between the suggested circuit and the traditional Converter. Another approach of integrating two boost cascaded converters is presented leading to a novel quadratic three-level converter. Compared to a quadratic boost converter with a single switch, the suggested topology's key benefit is a reduction in the total installed semiconductor power [3-4]. Other approaches include, introduction of a series of DC-DC converters built on the traditional Zeta-converter [5], two different switched inductor/switched capacitor architectures [6], continuous conduction and discontinuous conduction switching circuits [7], which hybrid circuit offer a large voltage gain while yet having relatively moderate voltage strains on the elements [8-9] are analyzed for DC-DC power conversion in high gain requirements. Further, these techniques applied to EV scenarios have got additional constraints and control requirements. A battery-powered e-rickshaw with regenerative braking is integrated with photovoltaic (PV) technology and extensively researched [10-12]. Without a middle DC- DC converter, the energy regeneration topology has operated satisfactorily with the single stage conversion topologies observed in [13-15]. However, these suffer from output voltage

FOREX Publication
Open Access | Rapid and quality publishing
International Journal of
Electrical and Electronics Research (IJEER)
Research Article | Volume 13, Issue 1 | Pages 171-177 | e-ISSN: 2347-470X

regulation issues. On the other hand, there are special control requirements at the DC- DC conversion stage for the motor pertaining to BLDC principle, which require that motor may be driven from zero speed using a sensor less control method based on line voltage [16-18]. In these cases, the sensor less drive and energy regeneration e-rickshaw system model are anticipated to be extremely durable, effective, and dependable [19-20].

Among the DC- DC converters available for power conversion with fuel cell powered BLDC drives, Luo converter has good gain and less voltage stress [21]. This converter could achieve non- inverting polarity, DC insulation from input to output, and capacity to buck-boost as well as constant output current. There are many improvements made to the LUO converter to improve its performance including modification of clamped capacitors for a high-gain DC-DC conversion [22-23], synthesized combination of inductors and capacitors to lift the input voltage to a higher value of the output voltage [24-25], addition of boosting (voltage multiplier) cell before the load to expand the voltage conversion ratio [26-27]. The application of these modifications dwelled in to improvement in one or combination of the following performance indicators which include extended voltage gain [28-29], low voltage stress on power switches [30-31], minimal capacitor stress and less component count [32]. With these identified possibilities and scope for enhanced DC-DC power conversion in fuel cell powered BLDC motor drive for EV applications, this paper proposed a combined LUO converter with voltage multiplier controlled for synchronized operation of converter stages to achieve reduced voltage stress across converter capacitors. Following are the novel contributions of the article for DC-DC conversion in fuel cell powered BLDC motor drive:

- Modification of LUO converter to enhance clamping capacitors voltage stress
- An additional voltage-gain expansion stage for achieving high voltage gain with reduced voltage stress across converter elements
- Synchronized operation of LUO boost conversion and gain expansion cell to achieve low input current ripple
- Improved switch utilization factor for improved efficiency and reduced voltage stress across the switches
- Synchronized phase shift control of boost switches for symmetrical voltage ripple sharing between gain expander capacitors

Rest of the paper is organized as follows. *Section 2* presents the topology and steady state operation of the proposed converter. *Section 3* presents mathematical analysis of converter output voltage, stress on components and efficiency of the converter. *Section 4* present simulation results and *section 5* presents conclusions.

2. ENHANCE LUO CONVERTER FOR DC-DC CONVERSION

2.1. Drive and Converter Topology

The topology of enhanced LUO converter-based fuel cell powered BLDC motor is presented in *Fig.1*. The constant input voltage is generated by the fuel cell for the current demand at the load terminals. The proposed enhanced LUO converter provides the gain to input voltage supplied by fuel cell. The converter has two stages of power conversion. Firstly, a non-isolated boost mode raises the voltage level to an intermediate level which is followed by a passive voltage boost cell consisting of voltage multiplier ladder network. The boosted voltage is then utilized to power BLDC motor through three-phase voltage source inverter. The rotor position is sensed for commutation of BLDC motor phase voltages. Rotor speed is sensed for determining the motor phase current magnitude required to maintain the speed at set reference value. This section presents the detailed working of enhanced LUO converter for voltage boost operation.

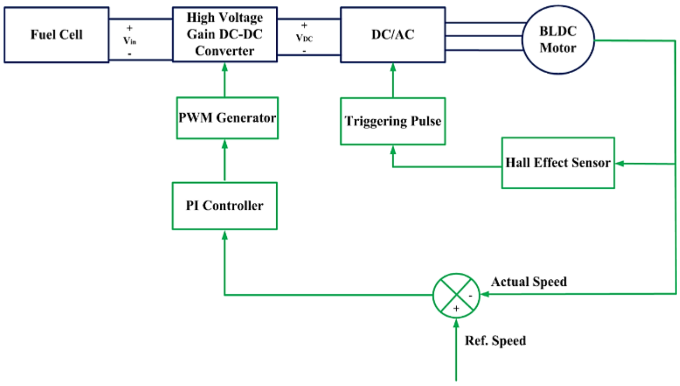

Figure 1. Enhanced LUO Converter based Fuel cell powered BLDC Drive Topology

The modified circuit for enhancing component stress performance for DC-DC power conversion is shown in *figure 2*. The principle of boost conversion is maintained along with reduction of voltage stress on clamping capacitors of the LUO converter. The gain is further raised by voltage multiplier, in which again symmetrical sharing of boosting operation is carried out using clamping bridge network. These aspects are detailed in the following sections.

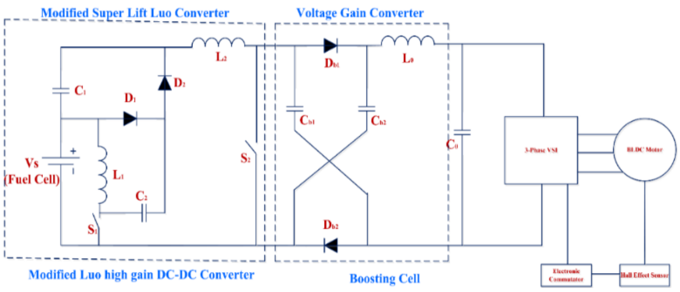

Figure 2. Enhanced LUO Converter for DC-DC power conversion in Fuel cell powered BLDC motor

2.2. Converter Operating Modes

To obtain the proposed converter an already existing high gain super lift LUO converter is enhanced with a diode-capacitor network as shown in *figure 3*. This resulted in low capacitive stress, extended voltage gain, low voltage stress on power switches, minimal capacitor stress and less component count. The voltage lift technique is implemented in the design of the

FOREX Publication
Open Access | Rapid and quality publishing
International Journal of
Electrical and Electronics Research (IJEER)
Research Article | Volume 13, Issue 1 | Pages 171-177 | e-ISSN: 2347-470X

four series Luo (DC-DC) converter, which increases the output voltage in arithmetic progression. The voltage gain transfer can be increased effectively by implementing the super-lift technique where the output voltage increases in a geometric progression. A high-frequency switch is combined with the diode-capacitor network in this circuit. The circuit has an input current with very small ripples and output voltage which is a multiple of the input voltage given to it. The capacitors in this circuit are not short-circuited by the switch and so the large discharge current stresses don't affect the working of the circuit unlike its operations in some similar available circuits. The efficiency of the circuit is high due to the lower presence of ripples. The combination of these two circuits results in the high gain enhanced Luo DC-DC converter.

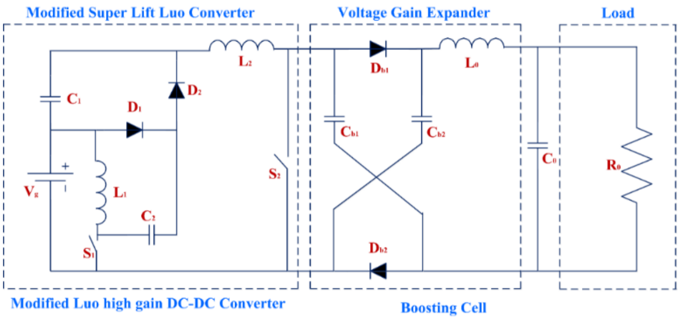

Figure 3. Circuit Diagram of Modified Luo Converter

The steady state operation of the converter for one switching cycle is described as follows:

Mode I: [0 < t < DTs]: In this period, switches S_1 and S_2 are turned ON as illustrated in *figure 4*. The input voltage Vg charges the inductor L_1. Similarly, inductor L_2 is charged by the input voltage and capacitor voltage VC1. The current through the inductors increases linearly. The diode D_1 is turned ON and diode D_2 is reversed biased due to the voltage across inductor L_2. Diodes (D_{b1} and D_{b2}) in boosting cell are in reverse biased state due to the voltage across inductor L_O. The load voltage V_O is the summation of the voltage across output inductor L_O and twice that of the voltage across the boosting capacitor.

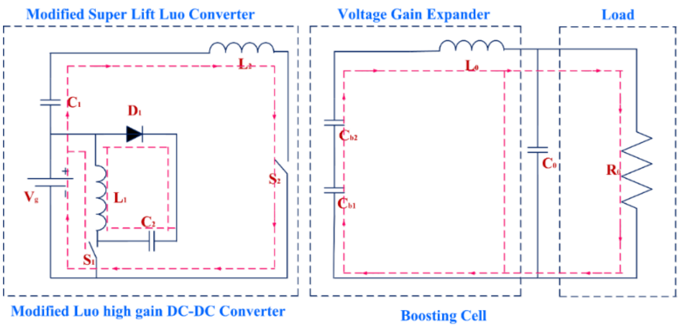

Figure 4. Equivalent Circuit Operation for Boosting Phase

Mode II: [DTs < t < Ts]: As shown in *figure 5,* switches S_1 and S_2 are in non- conducting state. The diode D_2 is forward biased due to the reverse polarity of the voltage across inductor L_2. The diode D_1 is in a reverse biased state. Diodes (D_{b1} and D_{b2}) in boosting cell are forward biased due to the negative polarity of the voltage across inductor L_O. The load voltage V_O is the summation of the voltage across output inductor L_O and voltage across the boosting capacitor.

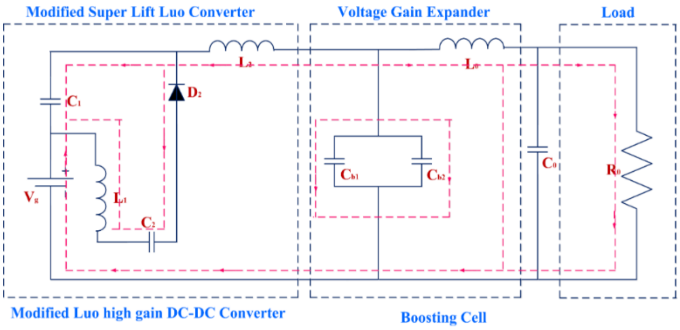

Figure 5. Equivalent Circuit Operation for Freewheeling Phase

Instantaneous values of the voltages across inductors L_1 and L_2 are presented in *figure 6* which aid in determining the steady state output voltage. Also, the voltage across load side filter inductor L_O is presented which determine the voltage across output filter capacitance which in turn responsible for output voltage ripple. The voltages across power switches S_1 and S_2 presented in *figure 6* depict the quantitative voltage stress to be borne by the respective switches. The higher stress is put on the multiplier network diodes which is observed from *figure 6.*

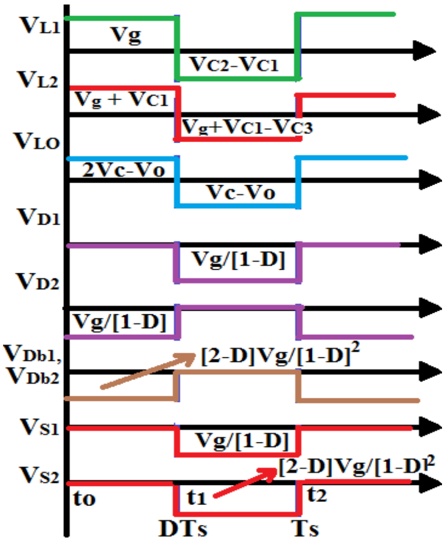

Figure 6. Gating signals and Switch voltages for one steady state cycle

3. CONVERTER ANALYSIS

The analysis of the enhanced Luo converter with respect to expression for output voltage and evaluation of converter efficiency is presented as follows:

3.1. Converter Output Voltage

The average voltage of the clamped capacitors in the boost conversion process as per the equivalent circuits presented in *figure 4* and *figure 5* are obtained as

$$V_{C1} = \frac{Vg}{D'} \tag{1}$$

$$V_{C2} = Vg \tag{2}$$

Also, the voltage clamped across multiplier cell capacitors is obtained as

$$V_{Cb1} = V_{Cb2} = (2-D)\frac{Vg}{D\prime^2} \tag{3}$$

The *equation (3)* determines the overall voltage gain to be

$$G_V = \frac{V_0}{V_g} = \frac{(2-D)(1+D)}{D\prime^2} \tag{4}$$

To generalize the voltage multiplication, the *equations (5), (6)* show the voltage gain when the number of boosting cells is even and odd respectively with m being the number of stages in voltage multiplier network.

$$G_{VE} = \frac{V_0}{V_g} = \frac{(2-D)[(M+1)-D]}{D\prime^2} \tag{5}$$

$$G_{VO} = \frac{V_0}{V_g} = \frac{(2-D)(M+D)}{D\prime^2} \tag{6}$$

The switch voltage stress is the maximum voltage to be blocked by the respective switch under OFF condition. From *figure 6* which depict the instantaneous switch voltages under steady state, the nominal switch stress is obtained as provided in the *equations (7)* and *(8)*

$$V_{S1} = \frac{Vg}{D\prime} \tag{7}$$

$$V_{S2} = \frac{(2-D)\,V_g}{D\prime^2} \tag{8}$$

Further, it is important to analyze the utilization factor of the switch which indicates the percentage contribution of switch in delivering power to load. The *equation (9)* presents the switch utilization factor in terms of total output power and power associated with switches. Transforming the quantities in terms of converter nominal parameters the switch utilization factor is obtained as given by *equation (10)*.

$$SUF = \frac{V_0 I_0}{V_{S1} I_{S1(rms)} + V_{S2} I_{S2(rms)}} \tag{9}$$

$$SUF_{ML} = \frac{G_V D\prime^3}{2D(2-D)+(1+D)\sqrt{D}} \tag{10}$$

3.2 Converter Efficiency

The efficiency analysis is carried out with the help of losses of the inductors, capacitors (passive elements) and diodes and switches (semiconductor devices) present in the converter.
The inductor loss (PL) is shown in *equation (11)* as:

$$P_L = [\frac{(1+D)I_0}{D\prime^2}]^2 R_{L1} + [\frac{(1+D)I_0}{D\prime}]^2 R_{L1} + [I_0]^2 R_{L0} \tag{11}$$

The switching losses and conduction loss in the switches S_1 and S_2 are shown in *equation (12)*.

$$P_{Sw} = \left[\frac{(1+D)I_0\sqrt{D}}{D'^2}\right]^2 R_{da1} + \left[\frac{2I_0 D\sqrt{D}}{D'}\right]^2 R_{da2} + \frac{f_s}{2}[(t_{r1}+t_{f1})I_{S1(avg)}V_{S1(max)} + (t_{r2}+t_{f2})I_{S1(avg)}V_{S1(max)} \tag{12}$$

The total diode losses PD of the proposed converter is obtained in the *equation (13)*.

$$P_D = \left\{2\left[\frac{(1+D)I_0}{D'}\right] + 4I_0 D\right\}V_f + \{2\left[\frac{(1+D)I_0\sqrt{1-D}}{D'^2}\right]^2 + 2[\frac{2I_0 D}{\sqrt{D\prime}}]^2\}R_f \tag{13}$$

$$P_C = \left\{2\left[\frac{(1+D)I_0}{D'}\right] + 2[\frac{I_0\sqrt{D}}{\sqrt{D\prime}}]^2\right\}R_{C(ESR)} \tag{14}$$

Using the *equations (11) – (14)* the total losses in converter are determined. Finally, the efficiency of the proposed converter is determined as

$$\%\,\eta = \frac{P_O}{P_L+P_C+P_D+P_{Sw}} \text{ X } 100 \tag{15}$$

4. SIMULATION RESULTS

The proposed DC-DC power conversion is simulated in MATLAB/SIMULINK environment. The operational parameters such as current in the inductors, voltage across capacitors and output voltage are analyzed for evaluating the performance of proposed converter. Simulation parameters for source, load, converter and filter aspects are presented in *table 1*. The necessary non-idealities in power switches and diodes, filter inductors and capacitors are considered for simulation study to analyze the realistic performance of the proposed converter. The simulation results for these quantities are presented in this section.

Table 1. Simulation Parameters

Component	Specifications
Load	45 V, 500 W
Fuel cell	Type: Hydrogen Voltage: 12 V Nominal Power: 550 W Fuel Rate: 0.74 m³/h Noise: 65 dB
Enhanced LUO Converter	Nominal Duty cycle: D = 0.25 Switching Frequency: 50 kHz Nominal Voltage gain = 3.88 Inductance: 1.25 mH Capacitance: 33 µF Power Switches: MOSFET, 100V, 10 A Power Diodes: 100 V, 10 A
Voltage Multiplier	Inductance: 0.36 mH Capacitance: 50 µF Power Diodes: 100 V, 10 A
Load side Filter	Inductance: .3 mH Capacitance: 100 µF

FOREX Publication
Open Access | Rapid and quality publishing

International Journal of
Electrical and Electronics Research (IJEER)
Research Article | Volume 13, Issue 1 | Pages 171-177 | e-ISSN: 2347-470X

Firstly, the voltage across the converter capacitors is analyzed to observed the reduction in voltage stress across capacitors and correspondingly on the power switches and diodes which are clamped by these capacitors. *Figure 7* which depict the voltages across C_1, C_2, C_{b1}, and C_{b2} confirm to the respective expressions presented in *section 3.1*. The voltage across C_1 is clamped to 11.8 V as seen from *Fig. 7(a)* which confirms to value obtained with *equation (1)*. The voltage across C_2 is observed to be 15.7V as seen from *figure 7(b)* which confirms to its value as determined from *equation (2)*. Also, the higher stress on the multiplier capacitors is evident from *Figure 7(c)*, which account for 35.55 V which also conform to their values as determined from *equation (3)*.

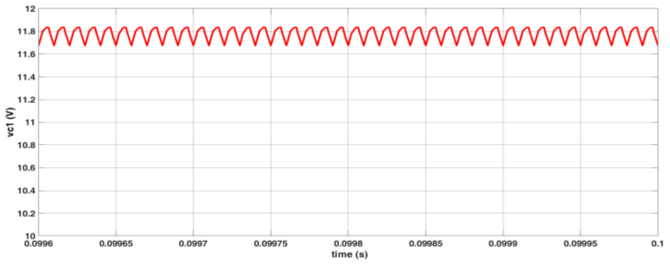

(a)

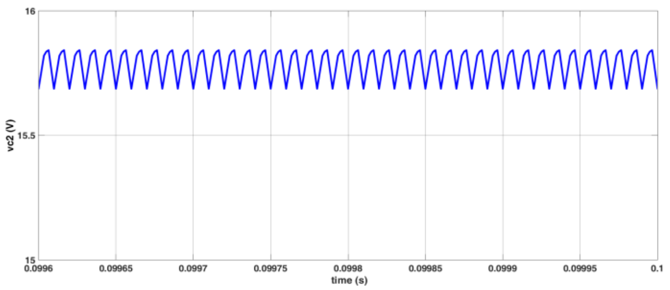

(b)

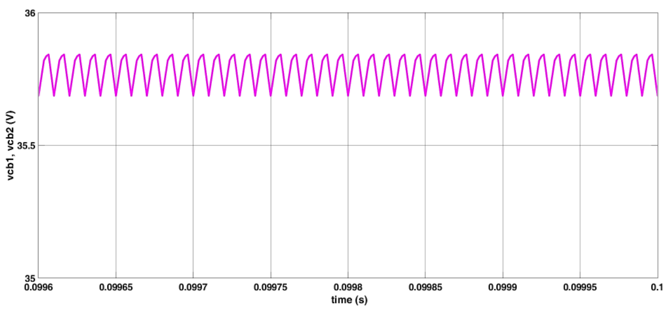

(c)

Figure 7. voltages across (a) C_1 (b) C_2, (c) C_{b1} and C_{b2}

Further, the current in the converter inductances L_1, L_2 and L_O are analyzed to verify the effect of reduced stress on the clamped capacitors. It is evident from *figure 8* that the ripple in inductor currents is reduced owing to the fact that the inductors are clamped to reduced voltages when the switches are ON and OFF condition in the enhanced Luo converter. However, the voltage boost is not compromised but boosted with the help of voltage gain expander. The output voltage as a result of the reduced stress in the components is depicted in *figure 9*. A reduced ripple in the output voltage is identified from *figure 9(a)*. Further, the transient settling time is observed to be 0.1 sec for sudden change in load. Also, owing to the voltage boost provided by the multiplier network the steady state value of the output voltage corresponds to the designed set value with very minimal regulation for load changes.

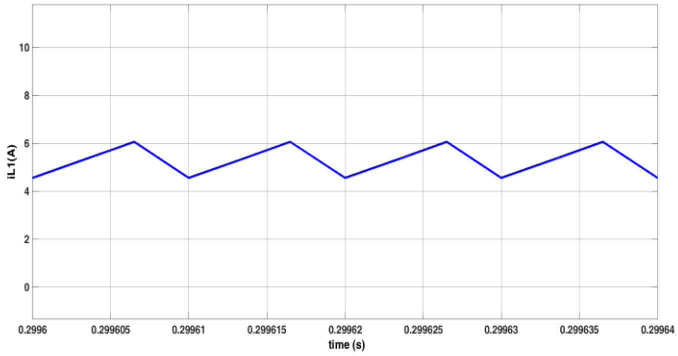

(a)

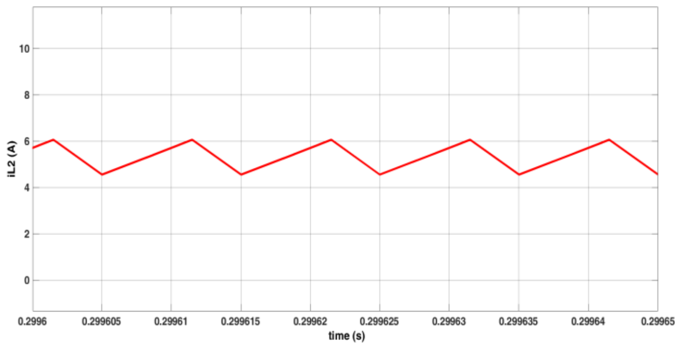

(b)

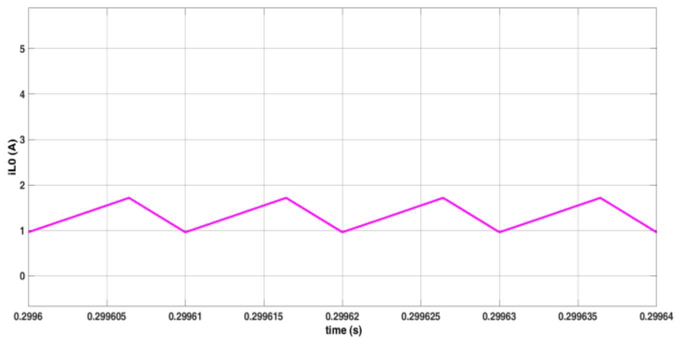

(c)

Fig. 8. Current in the converter inductors (a) L1, (b) L2, (c) LO

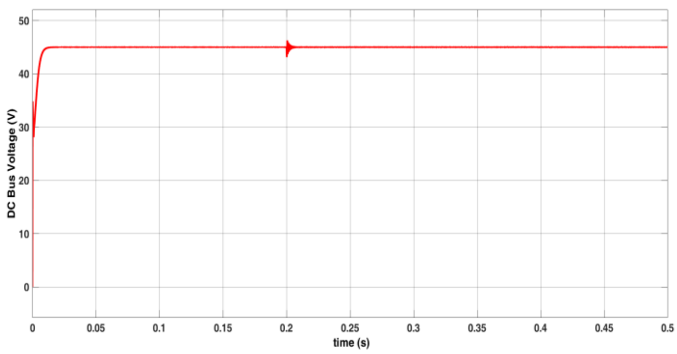

(a)

FOREX Publication
Open Access | Rapid and quality publishing

International Journal of
Electrical and Electronics Research (IJEER)
Research Article | Volume 13, Issue 1 | Pages 171-177 | e-ISSN: 2347-470X

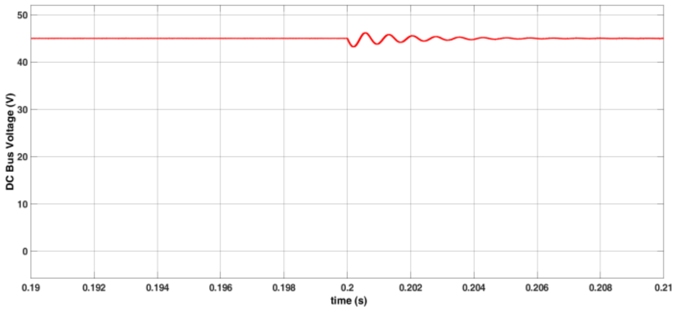

(b)

Figure 9. (a) Output voltage (b) transient state of output voltage for change in load

A comparative study is made in terms of structural parameters such as number of devices required for switching, multiplier, filter etc., and operational parameters such as duty cycle and voltage stress across the converter elements. These aspects are presented in *table 2*. The reduction in number of power switches required for power conversion is observed from the comparative analysis from *table 2*. Although it is observed that the conversion needed additional diodes and capacitor in comparison to existing converters, it is the reduction in operating duty by minimum 30 percent and reduction in voltage stress across capacitors by 41.67 percent resulting in reduction of size of required capacitors, switches and diodes. Also, the stringent voltage regulation provide by the converter makes the ease of control for the further stages of power conversion in BLDC motor control. Thus, the contribution enhanced the reliability of fuel cell powered BLDC motor control.

Table 2. Comparison of enhanced LUO converter with existing converters

Converter	Gain	No of Switches	No of Diodes	No of Inductors	No of Capacitors	Nominal Dutycycle	Capacitor Voltage stress
Proposed	$\frac{[2-D][1+D]}{D'^2}$	2	4	3	5	0.25	12 V, 15V, 36 V
Interleaved boost converter [26]	$\frac{[2+D]}{D'}$	3	3	3	3	0.7	17 V, 34V
Interleaved bidirectional converter [27]	$\frac{4}{D'}$	8	--	5	4	0.55	81V, 54 V 26 V
Voltage Quadruple Asymmetric converter [30]	$\frac{4}{D'}$	2	8	2	10	0.25	25V, 50 V
Two-switch SEPIC converter [31]	$\frac{2}{D'}$	3	3	3	3	0.7	17 V, 34V
Integrated LUO converter [32]	$\frac{[2+D]}{D'}$	2	3	3	3	0.5	25 V, 45V

5. CONCLUSIONS

The enhanced Luo converter with less capacitor voltage stress for fuel cell powered BLDC motor drive is proposed and analyzed. The feasibility of the converter is justified with achieved steady state voltages confining to the design values of 45 V at the output and 35.5 V across multiplier cell capacitor to produce required output voltage. The operational duty is confined only to 0.25 and voltage stress across capacitors is reduced by 41.67 percent. These indices present the enhanced performance of the converter in comparison to existing topologies for fuel cell powered BLDC drive front-end power conversion. Thus, the proposed converter for DC-DC conversion in fuel cell powered BLDC motor drive improved component stress handling performance and stringent output voltage. The further research work can implement novel control techniques such as model based current control to the proposed which improve dynamic performance of the converter for load changes and constraints of source dynamics.

REFERENCES

[1] Shindo, Yutaka, Makoto Yamanaka, and Hirotaka Koizumi. "Z-source DC-DC converter with cascade switched capacitor." IECON 2011-37th Annual Conference of the IEEE Industrial Electronics Society. IEEE, 2011.

[2] Prudente, Marcos, et al. "Voltage multiplier cells applied to non-isolated DC–DC converters." IEEE Transactions on Power Electronics 23.2 (2008): 871-887.

[3] De Novaes, Y. R., A. Rufer, and I. Barbi. "A new quadratic, three-level, dc/dc converter suitable for fuel cell applications." 2007 Power Conversion Conference-Nagoya. IEEE, 2007.

[4] Pan, Ching-Tsai, Chen-Feng Chuang, and Chia-Chi Chu. "A novel transformer-less adaptable voltage quadrupler DC converter with low switch voltage stress." IEEE Transactions on Power Electronics 29.9 (2013): 4787-4796.

[5] Axelrod, B., Y. Berkovich, and Y. Beck. "A family of modified zeta-converters with high voltage ratio for solar-pv systems." 2019 21st European Conference on Power Electronics and Applications (EPE'19 ECCE Europe). IEEE, 2019.

[6] Park, Yeji, et al. "Efficiency improvement of permanent magnet BLDC with Halbach magnet array for drone." IEEE Transactions on Applied Superconductivity 30.4 (2020): 1- 5

[7] Al-Adsani, Ahmad S., Michel E. AlSharidah, and Omid Beik. "BLDC motor drives: A single hall sensor method and a 160° commutation strategy." IEEE Transactions on Energy Conversion 36.3 (2020): 2025-2035.

[8] Tang, Bo-Hui, and Jie Wang. "A physics-based method to retrieve land surface temperature from MODIS daytime midinfrared data." IEEE Transactions onGeoscience and Remote Sensing 54.8 (2016): 4672-4679.

[9] Shanmugam, Sathish Kumar, et al. "Design and implementation of improved three port converter and B4-inverter fed brushless direct current motor drive system for industrial applications." IEEE Access 8 (2020): 149093-149112.

[10] Saha, Biswajit, Bhim Singh, and Aryadip Sen. "Solar PV Integration to E- Rickshaw with Regenerative Braking and Sensorless Control." IEEE Transactions on Industry Applications (2022).

[11] Sashidhar, S., V. Guru Prasad Reddy, and B. G. Fernandes. "A single-stage sensor less controlof a PV-based bore-well submersible BLDC motor." IEEE Journal of Emerging and Selected Topics in Power Electronics 7.2 (2018): 1173-1180.

[12] Sen, Aryadip, and Bhim Singh. "Peak current detection starting based position sensor less controlof BLDC motor drive for PV array fed irrigation pump." IEEE Transactions on Industry Applications 57.3 (2021): 2569-2577.

[13] Zhang, Haifeng, et al. "High-Precision Sensor less Optimal Commutation Deviation Correction Strategy of BLDC Motor with Asymmetric Back EMF." IEEE Transactions on Industrial Informatics 17.8 (2020): 5250-5259.

[14] Park, Joon Sung, et al. "Unbalanced ZCP compensation method for position sensor less BLDC motor." IEEE Transactions on Power Electronics 34.4 (2018):3020-3024.

[15] Yang, Lei, et al. "Virtual third harmonic back EMF-Based sensor less drive for high-speed BLDC motors considering machine parameter asymmetries." IEEE Transactions on Industry Applications 57.1 (2020): 306-315.

[16] Khazaee, Amir, et al. "MTPA strategy for direct torque control of brushless DC motor drive." IEEE Transactions on Industrial Electronics 68.8 (2020): 6692-6700.

[17] Nalli, R., Subbarao, K., Ramamoorthi, & Kirankumar, M. (2022). A new integrated ac-dc converter fed sensorless controlling technique for a 3-phase bldc motor. Journal of Engineering Science and Technology, 17(3), 2080–2094.

[18] Kolluru, A. K., & Malligunta, K. K. (2022). Fuzzy Controller Based DTC of SRM Drive Fed by Common High Side Asymmetric Switch Converter. International Journal of Electrical and Computer Engineering Systems, 13(8), 701–708. https://doi.org/10.32985/ijeces.13.8.10

[19] Zhang, Yun, et al. "DC–DC boost converter with a wide input range and highvoltage gain for fuelcell vehicles." IEEE Transactions on Power Electronics 34.5(2018): 4100-4111

[20] Fang Lin Luo, Hong Ye "Positive output super-lift converters," IEEE Journal, DOI 10.1109/TPEL.2002.807198.

[21] Fang Lin Luo "Investigation on Split-Capacitors applied in positive output Super-Lift Luo- Converters," IEEE Journal, DOI 10.1109/CCDC.2011.5968686.

[22] Jing LI, and Jinjun Liu "Modelling and analysis of elementary positive output and super lift converter feeding constant power load," 2016 IEEE 2nd Annual Southern Power Electronics Conference (SPEC), ISBN: 978-1-5090-1546-7, INSPEC: 16666525

[23] S. N. Choudhary and Elangovan D, "High gain, naturally clamped Dc to Dc converter for X-ray application," 2016 International Conference on Computation of Power, Energy Information and Communication (ICCPEIC), Chennai, 2016, pp. 587-592, DOI: 10.1109/ICCPEIC.2016.7557298.

[24] Chaitanya Pansare, Shailendra Sharma, Chinmay Jain, Rakesh Saxena, "Analysis of a modified positive output Luo converter and its application," 2017 IEEE Industry Applications Society Annual Meeting, DOI: 1/10/2017, ISBN:978-1-5090-4894-6, INSPEC:17354718

[25] Fanglin Luo, "Investigation of split capacitors applied in positive output super luo converters," 2011 Chinese Control and Decision Conference (CCDC), ISBN: 978-1-4244- 8738-7, INSPEC: 12143980

[26] Sreelatha E, Pandian A, Reddy CR, Kumar MK, Kotb H, M. AboRas K, et al. (2024) An efficient high-gain bidirectional interleaved boost converter for PV integration to DC microgrid. PLoS ONE 19(5): e0301522. https://doi.org/10.1371/journal.pone.0301522

[27] Kumar Kolluru A, Malligunta KK, Teja SR, Reddy CR, Alqahtani M and Khalid M (2023) A novel controller for PV-fed water pumping optimization system driven by an 8/6 pole SRM with asymmetrical converter. Front. Energy Res. 11:1205704. doi: 10.3389/fenrg.2023.1205704

[28] Ramineni, P., Pandian, A., Kumar, M. K., & Sundaram, K. M. (2022). Improved operation of Li-ion battery with supercapacitor realized to solar-electric vehicle. Energy Reports, 8, 256–264. https://doi.org/10.1016/j.egyr.2022.10.191

[29] Yi-feng Wang, Li-kun Xue, Cheng-shan Wang., "Interleaved High-Conversion-Ratio Bidirectional DC-DC Converter for Distributed Energy-Storage Systems — Circuit Generation, Analysis and Design," IEEE Trans. Power Electron, 2015; 31(8): 5547-5561.

[30] M. R. Mohammed, A. S. Al-Sumaiti, A. R. Beig, K. Al Hosani and C. Wang, "A common grounded voltage quadrupler ASL/PSC hybrid converter with reduced voltage stress", IEEE Trans. Ind. Electron., vol. 71, no. 5, pp. 4773-4784, May 2024.

[31] S. Selvam, M. Sannasy and M. Sridharan, "Analysis and design of two-switch enhanced gain SEPIC converter", IEEE Trans. Ind. Appl., vol. 59, no. 3, pp. 3552-3561, May/Jun. 2023.

[32] A. Prajapati and K. Chaudhary, "Analysis and Design of Integrated Boost-Luo Converter with Reduced Voltage Stress for Renewable Application," in IEEE Journal of Emerging and Selected Topics in Industrial Electronics, vol. 5, no. 4, pp. 1613-1624, Oct. 2024, doi: 10.1109/JESTIE.2024.3365388.